

# Polarization of domain boundaries in SrTiO<sub>3</sub> studied by layer group and order-parameter symmetry

W. Schranz <sup>\*</sup>, C. Schuster, and A. Tröster

University of Vienna, Faculty of Physics, Boltzmanngasse 5, 1090 Wien, Austria

I. Rychetsky

Institute of Physics, Academy of Sciences of the Czech Republic, Na Slovance 2, 18221 Prague 8, Czech Republic

 (Received 7 August 2020; revised 29 September 2020; accepted 20 October 2020; published 3 November 2020)

Based on a recently developed combination of layer group analysis with order-parameter symmetry, we study the polarity of antiphase domain boundaries (APBs) and ferroelastic twin boundaries (TBs) in SrTiO<sub>3</sub>. In addition to the celebrated layer group analysis of domain twins, the present method allows us to investigate tensor properties of domain walls also for the case where order-parameter variables other than the spontaneous ones are active. We find that antiphase boundaries in SrTiO<sub>3</sub> can carry a polarization if in addition to the spontaneous order parameter  $(0, 0, \phi_s)$  a second component, i.e.,  $(\phi_1, 0, \phi_s)$ , develops within the domain wall. This result, which is solely based on symmetry arguments, strongly suggests that polarization in APBs is possible if a phase transition from an Ising-type wall to a Néel- or Bloch-like wall occurs. This is in very good agreement with previous calculations based on Landau-Ginzburg free energy expansions including biquadratic  $(\propto P_i P_j \phi_k \phi_l)$  [A. K. Tagantsev *et al.* *Phys. Rev. B* **64**, 224107 (2001)] and flexoelectric  $(\propto P_k \frac{\partial u_{ij}}{\partial x_l})$  coupling terms [A. N. Morozovska *et al.* *Phys. Rev. B* **85**, 094107 (2012)]. The present results also unveil a close connection between the recently discovered macroscopic polarization in antiferrodistortive cycloids of ferroelastic domain walls of SrTiO<sub>3</sub> and a mechanism for explaining polarization of APBs.

DOI: [10.1103/PhysRevB.102.184101](https://doi.org/10.1103/PhysRevB.102.184101)

## I. INTRODUCTION

Since the discovery of novel domain wall (DW) properties, like conducting DWs in insulating BaTiO<sub>3</sub> [1] or polarity in nonpolar perovskites CaTiO<sub>3</sub> [2–4], SrTiO<sub>3</sub> [5], and LaAlO<sub>3</sub> [6], domain walls have attracted much attention [7] for their potential use in nanoelectronic devices [8]. Translational antiphase boundaries below antiferrodistortive phase transitions have been considered specifically interesting due to their ability to carry DW polarization [9]. In the antiferroelectric PbZrO<sub>3</sub> there is experimental evidence that antiphase boundaries (APBs) are polar [10,11]. Moreover, based on *ab initio* calculations the authors claimed [10] that the DW polarization there can be switched, supporting the ferroelectric nature of the APB. Since APBs are an order of magnitude thinner (few unit cells) than magnetic domain walls, this would make APBs enormously interesting for building high-density (nanoferroelectric) memories.

SrTiO<sub>3</sub> is another example where polarization inside APBs was predicted by Tagantsev *et al.* [12] below  $\sim 40$  K. These authors have created the terms “easy” and “hard” APBs, for domain walls perpendicular or parallel to the tetragonal  $c$  axis, respectively. They found [12] that “easy” APBs are of Ising type (only one component of the order parameter is involved) with zero polarization inside the wall, whereas the order-parameter profile of “hard” APBs develops already below  $T_c = 105$  K a second component, like in Néel walls. The

authors have further shown that “hard” APBs can host a polarization component  $P_3$  (parallel to the tetragonal  $c$  axis) as a result of a local ferroelectric transition below  $\approx 40$  K, which is induced by biquadratic coupling terms  $b_{ijkl} P_i P_j \phi_k \phi_l$  between the primary order parameter (OP)  $\phi_k$  and the polarization  $P_i$  in the free energy expansion.

Later it was shown [9] that flexoelectric coupling terms  $f_{ijkl} P_k \frac{\partial u_{ij}}{\partial x_l}$  between the polarization and the strain-gradient  $\nabla u_{ij}$  can induce a DW polarization in SrTiO<sub>3</sub> already below  $T_c = 105$  K.

*Ab initio* calculations [13] have confirmed the existence of a polarization component  $P_3$  in “hard” APBs of SrTiO<sub>3</sub>, though obtaining a different structure of the DWs (nearly Ising type) as compared to the results from a phenomenological approach [9] including flexoelectric coupling terms, which were found to be of Néel type.

In line with earlier work of Eliseev *et al.* [14], Schiaffino and Stengel [15] identified two further mechanisms that contribute to DW polarity in ferroelastic twin walls of SrTiO<sub>3</sub>: A direct “rotopolar” coupling of the type  $W_{rs} P_r (\frac{\partial \phi_r}{\partial s} \phi_s - \frac{\partial \phi_s}{\partial r} \phi_r)$  ( $\mathbf{r}$  is parallel to the twin wall and  $\mathbf{s}$  is perpendicular to the twin wall) and a trilinear coupling  $\propto P_r u_3^{Ti} \phi_s$  ( $s$  points along the DW normal) that is mediated by the antiferroelectric displacements  $u_3^{Ti}$  of the Ti atoms. Such terms break the macroscopic inversion symmetry and allow for a macroscopic polarization of a system of parallel twin walls in SrTiO<sub>3</sub>, thus opening a promising perspective for DW engineering. Interestingly enough, the present analysis shows that similar coupling terms are important for the description of polarization in APBs also.

<sup>\*</sup>wilfried.schranz@univie.ac.at

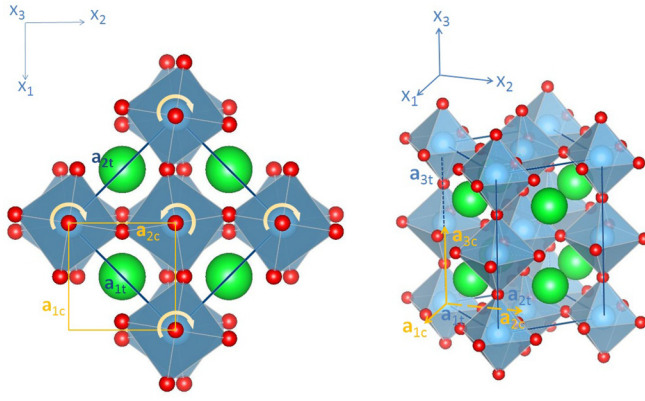


FIG. 1. Relation between cubic  $Pm\bar{3}m$  and tetragonal  $I4/mcm$  unit cells of  $\text{SrTiO}_3$ . Note that we are working entirely in the cubic reference frame, i.e.,  $(x_1, x_2, x_3)$ . Sometimes we use also the notation  $(x_c, y_c, z_c)$ . The origin  $(0,0,0)$  is chosen at Ti atoms (light blue), Sr atoms (green) at  $(\frac{a}{2}, \frac{a}{2}, \frac{a}{2})$ , and O atoms (red) at  $(\frac{a}{2}, 0, 0)$  and equivalent positions. This and similar drawings were made with VESTA [33].

Although predicted by various theoretical methods, up to now there exists no direct measurement of a DW polarization in  $\text{SrTiO}_3$ . However, experimental observations of piezoelectric resonance [5] starting below  $\approx 80$  K and becoming stronger below  $\approx 40$  K have been interpreted as a signature of the polar character of the DWs. Perhaps the most direct proof for the polar character of twin boundaries below  $\approx 40$  K in  $\text{SrTiO}_3$  comes from recent measurements [16] of the current flow from individual twin walls in response to an applied local stress.

From what is said above, it is clear that DWs in  $\text{SrTiO}_3$  are interesting candidates for future applications. Given the above-mentioned variety of coupling mechanisms for DW polarization, we felt it is the right time to apply our recently developed methods [17] to  $\text{SrTiO}_3$ . In the present work we show that a combination of OP symmetries with layer group analysis [18] yields valuable information on the symmetry-allowed polarization components of individual DWs. In addition we identify the minimal coupling terms which are needed for modeling polarity of translational APBs and ferroelastic twin boundaries (TBs) of  $\text{SrTiO}_3$ . The present method can be useful to link microscopic DW theories to phenomenological models.

## II. GROUP-THEORETICAL CONSIDERATIONS OF THE PHASE TRANSITION IN $\text{SrTiO}_3$

$\text{SrTiO}_3$  undergoes an antiferrodistortive structural phase transition [19] at  $T_c = 105$  K from a simple cubic room-temperature phase with space group  $G = Pm\bar{3}m$  to a tetragonal phase  $F = I4/mcm$ , where  $F < G$ . The cubic space group is symmorphic, i.e.,  $G = \cup_{g \in Pm\bar{3}m} \mathbf{T}^c(g|000)$ , where  $\mathbf{T}^c = \{n_1 \mathbf{a}_1^c + n_2 \mathbf{a}_2^c + n_3 \mathbf{a}_3^c\}$  is the translation group with  $\mathbf{a}_1^c = (a, 0, 0)$ ,  $\mathbf{a}_2^c = (0, a, 0)$ , and  $\mathbf{a}_3^c = (0, 0, a)$ , with  $a = 3.905$  Å. The phase transition is due to static rotations  $(0, 0, \phi_3)$  of the  $\text{TiO}_6$  octahedra around the tetragonal  $c$ -axis, which are alternating  $(0, 0, \pm\phi_3)$  along all three cubic directions (see Fig. 1 for the present setting). Due to these staggered

rotations the translations  $(2n_1 + 1)(a, 0, 0)$ ,  $(2n_2 + 1)(0, a, 0)$ , and  $(2n_3 + 1)(0, 0, a)$  are lost.

The tetragonal lattice is then related to the cubic one (Fig. 1) as  $\mathbf{T}^t = \{\mathbf{a}_1^c + \mathbf{a}_2^c, -\mathbf{a}_1^c + \mathbf{a}_2^c, \mathbf{a}_2^c + \mathbf{a}_3^c\} = \{(a, a, 0), (-a, a, 0), (0, a, a)\}$ . The phase transition occurs at the  $R$  point of the Brillouin zone, with the active irrep  $R_4^+$  and  $\mathbf{k}_R = \frac{2\pi}{a}(\frac{1}{2} \frac{1}{2} \frac{1}{2})$ . Since we perform the calculations entirely in order-parameter space, we give the explicit form of  $R_4^+$  in Table I.

Due to the symmetry reduction at the phase transition, the distorted phase can appear in  $N = 6$  domain states (DSs), which can be calculated from the following simple formula [20]:

$$N = \frac{|G|}{|F|} \times \frac{|V_F|}{|V_G|} = 3 \times 2 = 6, \quad (1)$$

where  $|G|$ ,  $|F|$  is the order of the point group of  $G$  and  $F$ , respectively and  $|V_G|$ ,  $|V_F|$  are the volumes of the primitive unit cells of the groups  $G$  and  $F$ , respectively. In the present case  $|G| = 48$ ,  $|F| = 16$  and the tetragonal primitive unit cell is twice the cubic unit cell, hence  $N = 6$ .

We can therefore designate the six DSs of  $\text{SrTiO}_3$  as  $1_1, 1_2, 2_1, 2_2, 3_1, 3_2$ , where the first number denotes the three different orientation states 1, 2, 3 (Fig. 2) and the subscript specifies one of the two different translational states within each orientation state.

In Fig. 3 the six domain states are represented as points in order-parameter space, i.e.,  $1_1 = (\phi, 0, 0)$ ,  $2_1 = (0, \phi, 0)$ ,  $3_1 = (0, 0, \phi)$ , etc. The corresponding domain walls which connect the various DSs are shown as lines.

Let us denote the symmetry group of  $1_1 = (\phi, 0, 0)$  by  $F_1$ . These are all symmetry elements of  $Pm\bar{3}m$ , that leave  $(\phi, 0, 0)$  invariant. Using Table I we find

$$F_1 = \mathbf{T}^t \{ (1/000) (2_x/000) (2_y/00a) (2_z/00a) (4_x^+/000) (4_x^-/000) (2_{yz}/00a) (2_{y\bar{z}}/00a) (\bar{1}/000) (m_x/000) (m_y/00a) (m_z/00a) (S_{4x}^-/000) (S_{4x}^+/000) (m_{yz}/00a) (m_{y\bar{z}}/00a) \}. \quad (2)$$

All other DSs are obtained by application of the symmetry elements of  $G/F_1$ , i.e., those which are lost at the transition. They can also be easily found from Table I by grouping the symmetry elements which transform  $(\phi, 0, 0)$  into  $(-\phi, 0, 0)$ ,  $(0, \phi, 0)$ , etc. Table II shows the corresponding decomposition of  $G = Pm\bar{3}m$  into left cosets of  $F_1 = I4_x/m_x c_{yz} m_y$ .

## III. SYMMETRY OF DOMAIN PAIRS AND DOMAIN TWINS

In this section we present the main steps for the calculation of all nonequivalent domain twins (DTs) for  $\text{SrTiO}_3$ . We start with the calculation of all nonequivalent domain pairs (DPs). DPs represent an intermediate step [21] between DSs and DTs. For the present purpose, we will consider *unordered* DPs, which we denote as

$$\{S_i, S_j\} = \{S_j, S_i\}, \quad i \neq j (i, j = 1-6). \quad (3)$$

TABLE I. Active irreducible representation  $R_4^+$  of the cubic space group  $Pm\bar{3}m = O_h^1$ .

(1/000)	(2 <sub>x</sub> /000)	(2 <sub>y</sub> /000)	(2 <sub>z</sub> /000)	(C <sub>31</sub> <sup>-</sup> /000)	(C <sub>32</sub> <sup>-</sup> /000)	(C <sub>33</sub> <sup>-</sup> /000)	(C <sub>34</sub> <sup>-</sup> /000)	OP
(x y z)	(x $\bar{y}$ $\bar{z}$ )	( $\bar{x}$ y $\bar{z}$ )	( $\bar{x}$ $\bar{y}$ z)	(y z x)	(y $\bar{z}$ $\bar{x}$ )	( $\bar{y}$ z $\bar{x}$ )	( $\bar{y}$ $\bar{z}$ x)	
$\begin{pmatrix} 1 & 0 & 0 \\ 0 & 1 & 0 \\ 0 & 0 & 1 \end{pmatrix}$	$\begin{pmatrix} 1 & 0 & 0 \\ 0 & -1 & 0 \\ 0 & 0 & -1 \end{pmatrix}$	$\begin{pmatrix} -1 & 0 & 0 \\ 0 & 1 & 0 \\ 0 & 0 & -1 \end{pmatrix}$	$\begin{pmatrix} -1 & 0 & 0 \\ 0 & -1 & 0 \\ 0 & 0 & 1 \end{pmatrix}$	$\begin{pmatrix} 0 & 1 & 0 \\ 0 & 0 & 1 \\ 1 & 0 & 0 \end{pmatrix}$	$\begin{pmatrix} 0 & 1 & 0 \\ 0 & 0 & -1 \\ -1 & 0 & 0 \end{pmatrix}$	$\begin{pmatrix} 0 & -1 & 0 \\ 0 & 0 & 1 \\ -1 & 0 & 0 \end{pmatrix}$	$\begin{pmatrix} 0 & -1 & 0 \\ 0 & 0 & -1 \\ 1 & 0 & 0 \end{pmatrix}$	$\phi_1$ $\phi_2$ $\phi_3$
(C <sub>31</sub> <sup>+</sup> /000)	(C <sub>34</sub> <sup>+</sup> /000)	(C <sub>32</sub> <sup>+</sup> /000)	(C <sub>33</sub> <sup>+</sup> /000)	(2 <sub><math>\bar{y}</math></sub> /000)	(4 <sub>z</sub> <sup>+</sup> /000)	(4 <sub>z</sub> <sup>-</sup> /000)	(2 <sub>xy</sub> /000)	OP
(z x y)	(z $\bar{x}$ $\bar{y}$ )	( $\bar{z}$ x $\bar{y}$ )	( $\bar{z}$ $\bar{x}$ y)	( $\bar{y}$ $\bar{x}$ z)	( $\bar{y}$ x z)	(y $\bar{x}$ z)	(y x $\bar{z}$ )	
$\begin{pmatrix} 0 & 0 & 1 \\ 1 & 0 & 0 \\ 0 & 1 & 0 \end{pmatrix}$	$\begin{pmatrix} 0 & 0 & 1 \\ -1 & 0 & 0 \\ 0 & -1 & 0 \end{pmatrix}$	$\begin{pmatrix} 0 & 0 & -1 \\ 1 & 0 & 0 \\ 0 & -1 & 0 \end{pmatrix}$	$\begin{pmatrix} 0 & 0 & -1 \\ -1 & 0 & 0 \\ 0 & 1 & 0 \end{pmatrix}$	$\begin{pmatrix} 0 & -1 & 0 \\ -1 & 0 & 0 \\ 0 & 0 & -1 \end{pmatrix}$	$\begin{pmatrix} 0 & -1 & 0 \\ 1 & 0 & 0 \\ 0 & 0 & 1 \end{pmatrix}$	$\begin{pmatrix} 0 & 1 & 0 \\ -1 & 0 & 0 \\ 0 & 0 & 1 \end{pmatrix}$	$\begin{pmatrix} 0 & 1 & 0 \\ 1 & 0 & 0 \\ 0 & 0 & -1 \end{pmatrix}$	$\phi_1$ $\phi_2$ $\phi_3$
(2 <sub>y<math>\bar{z}</math></sub> /000)	(2 <sub>yz</sub> /000)	(4 <sub>x</sub> <sup>+</sup> /000)	(4 <sub>x</sub> <sup>-</sup> /000)	(2 <sub><math>\bar{x}</math></sub> /000)	(4 <sub>y</sub> <sup>+</sup> /000)	(2 <sub>zx</sub> /000)	(4 <sub>y</sub> <sup>-</sup> /000)	OP
( $\bar{x}$ $\bar{z}$ $\bar{y}$ )	( $\bar{x}$ z y)	(x $\bar{z}$ y)	(x z $\bar{y}$ )	( $\bar{z}$ $\bar{y}$ $\bar{x}$ )	( $\bar{z}$ y x)	(z $\bar{y}$ x)	(z y $\bar{x}$ )	
$\begin{pmatrix} -1 & 0 & 0 \\ 0 & 0 & -1 \\ 0 & -1 & 0 \end{pmatrix}$	$\begin{pmatrix} -1 & 0 & 0 \\ 0 & 0 & 1 \\ 0 & 1 & 0 \end{pmatrix}$	$\begin{pmatrix} 1 & 0 & 0 \\ 0 & 0 & -1 \\ 0 & 1 & 0 \end{pmatrix}$	$\begin{pmatrix} 1 & 0 & 0 \\ 0 & 0 & 1 \\ 0 & -1 & 0 \end{pmatrix}$	$\begin{pmatrix} 0 & 0 & -1 \\ 0 & -1 & 0 \\ -1 & 0 & 0 \end{pmatrix}$	$\begin{pmatrix} 0 & 0 & -1 \\ 0 & 1 & 0 \\ 1 & 0 & 0 \end{pmatrix}$	$\begin{pmatrix} 0 & 0 & 1 \\ 0 & -1 & 0 \\ 1 & 0 & 0 \end{pmatrix}$	$\begin{pmatrix} 0 & 0 & 1 \\ 0 & 1 & 0 \\ -1 & 0 & 0 \end{pmatrix}$	$\phi_1$ $\phi_2$ $\phi_3$
( $\bar{1}$ /000)	(m <sub>x</sub> /000)	(m <sub>y</sub> /000)	(m <sub>z</sub> /000)	(S <sub>61</sub> <sup>+</sup> /000)	(S <sub>62</sub> <sup>+</sup> /000)	(S <sub>63</sub> <sup>+</sup> /000)	(S <sub>64</sub> <sup>+</sup> /000)	OP
( $\bar{x}$ $\bar{y}$ $\bar{z}$ )	( $\bar{x}$ y z)	(x $\bar{y}$ z)	(x y $\bar{z}$ )	( $\bar{y}$ $\bar{z}$ $\bar{x}$ )	( $\bar{y}$ z x)	(y $\bar{z}$ x)	(y z $\bar{x}$ )	
$\begin{pmatrix} 1 & 0 & 0 \\ 0 & 1 & 0 \\ 0 & 0 & 1 \end{pmatrix}$	$\begin{pmatrix} 1 & 0 & 0 \\ 0 & -1 & 0 \\ 0 & 0 & -1 \end{pmatrix}$	$\begin{pmatrix} -1 & 0 & 0 \\ 0 & 1 & 0 \\ 0 & 0 & -1 \end{pmatrix}$	$\begin{pmatrix} -1 & 0 & 0 \\ 0 & -1 & 0 \\ 0 & 0 & 1 \end{pmatrix}$	$\begin{pmatrix} 0 & 1 & 0 \\ 0 & 0 & 1 \\ 1 & 0 & 0 \end{pmatrix}$	$\begin{pmatrix} 0 & 1 & 0 \\ 0 & 0 & -1 \\ -1 & 0 & 0 \end{pmatrix}$	$\begin{pmatrix} 0 & -1 & 0 \\ 0 & 0 & 1 \\ -1 & 0 & 0 \end{pmatrix}$	$\begin{pmatrix} 0 & -1 & 0 \\ 0 & 0 & -1 \\ 1 & 0 & 0 \end{pmatrix}$	$\phi_1$ $\phi_2$ $\phi_3$
(S <sub>61</sub> <sup>-</sup> /000)	(S <sub>64</sub> <sup>-</sup> /000)	(S <sub>62</sub> <sup>-</sup> /000)	(S <sub>63</sub> <sup>-</sup> /000)	(m <sub><math>\bar{y}</math></sub> /000)	(S <sub>4z</sub> <sup>-</sup> /000)	(S <sub>4z</sub> <sup>+</sup> /000)	(m <sub>xy</sub> /000)	OP
( $\bar{z}$ $\bar{x}$ $\bar{y}$ )	( $\bar{z}$ x y)	(z $\bar{x}$ y)	(z x $\bar{y}$ )	(y x z)	(y $\bar{x}$ $\bar{z}$ )	( $\bar{y}$ x $\bar{z}$ )	( $\bar{y}$ $\bar{x}$ z)	
$\begin{pmatrix} 0 & 0 & 1 \\ 1 & 0 & 0 \\ 0 & 1 & 0 \end{pmatrix}$	$\begin{pmatrix} 0 & 0 & 1 \\ -1 & 0 & 0 \\ 0 & -1 & 0 \end{pmatrix}$	$\begin{pmatrix} 0 & 0 & -1 \\ 1 & 0 & 0 \\ 0 & -1 & 0 \end{pmatrix}$	$\begin{pmatrix} 0 & 0 & -1 \\ -1 & 0 & 0 \\ 0 & 1 & 0 \end{pmatrix}$	$\begin{pmatrix} 0 & -1 & 0 \\ -1 & 0 & 0 \\ 0 & 0 & -1 \end{pmatrix}$	$\begin{pmatrix} 0 & -1 & 0 \\ 1 & 0 & 0 \\ 0 & 0 & 1 \end{pmatrix}$	$\begin{pmatrix} 0 & 1 & 0 \\ -1 & 0 & 0 \\ 0 & 0 & 1 \end{pmatrix}$	$\begin{pmatrix} 0 & 1 & 0 \\ 1 & 0 & 0 \\ 0 & 0 & -1 \end{pmatrix}$	$\phi_1$ $\phi_2$ $\phi_3$
(m <sub>y<math>\bar{z}</math></sub> /000)	(m <sub>yz</sub> /000)	(S <sub>4x</sub> <sup>-</sup> /000)	(S <sub>4x</sub> <sup>+</sup> /000)	(m <sub>z<math>\bar{x}</math></sub> /000)	(S <sub>4y</sub> <sup>+</sup> /000)	(m <sub>zx</sub> /000)	(S <sub>4y</sub> <sup>-</sup> /000)	OP
(x z y)	(x $\bar{z}$ $\bar{y}$ )	( $\bar{x}$ z $\bar{y}$ )	( $\bar{x}$ $\bar{z}$ y)	(z y x)	(z $\bar{y}$ $\bar{x}$ )	( $\bar{z}$ y $\bar{x}$ )	( $\bar{z}$ $\bar{y}$ x)	
$\begin{pmatrix} -1 & 0 & 0 \\ 0 & 0 & -1 \\ 0 & -1 & 0 \end{pmatrix}$	$\begin{pmatrix} -1 & 0 & 0 \\ 0 & 0 & 1 \\ 0 & 1 & 0 \end{pmatrix}$	$\begin{pmatrix} 1 & 0 & 0 \\ 0 & 0 & -1 \\ 0 & 1 & 0 \end{pmatrix}$	$\begin{pmatrix} 1 & 0 & 0 \\ 0 & 0 & 1 \\ 0 & -1 & 0 \end{pmatrix}$	$\begin{pmatrix} 0 & 0 & -1 \\ 0 & -1 & 0 \\ -1 & 0 & 0 \end{pmatrix}$	$\begin{pmatrix} 0 & 0 & -1 \\ 0 & 1 & 0 \\ 1 & 0 & 0 \end{pmatrix}$	$\begin{pmatrix} 0 & 0 & 1 \\ 0 & -1 & 0 \\ 1 & 0 & 0 \end{pmatrix}$	$\begin{pmatrix} 0 & 0 & 1 \\ 0 & 1 & 0 \\ -1 & 0 & 0 \end{pmatrix}$	$\phi_1$ $\phi_2$ $\phi_3$

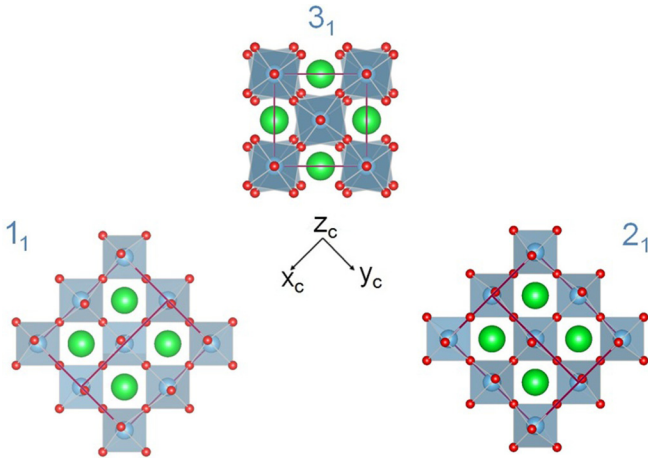
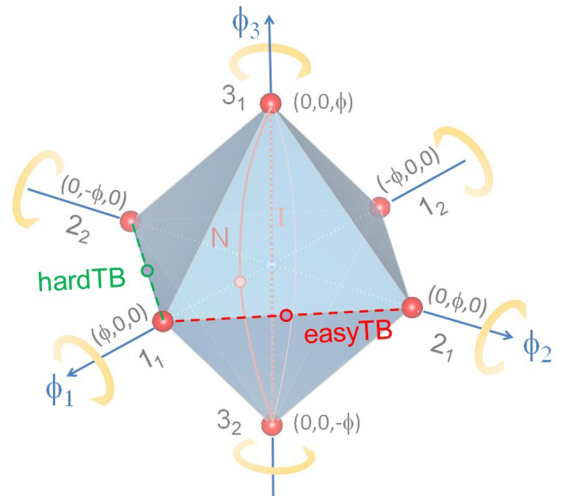
FIG. 2. Scheme of the 3 orientational domain states  $1_1, 2_1, 3_1$  of  $\text{SrTiO}_3$ . The cubic reference system ( $x_c, y_c, z_c$ ) is depicted in the center.FIG. 3. Six domain states of  $\text{SrTiO}_3$  in order-parameter space. The dashed and full lines indicate some selected domain wall trajectories between translational domain states  $3_1, 3_2$  (pink) and orientational domain states  $1_1, 2_1$  (violet). I = Ising wall, N = Néel wall, TB = twin boundary.

TABLE II. Decomposition of  $G = Pm\bar{3}m$  into left cosets of  $F_1 = I4_x/m_x c_{yz} m_y$ , yielding six DSs of SrTiO<sub>3</sub>.

$G = Pm\bar{3}m$	$g_j \in G \setminus F_1$	$1_1 \rightarrow S_j$ ( $S=1, 2, 3$ ) ( $j=1, 2$ )	DSs in OP space	Symmetry group	Hermann-Mauguin symbol
$G =$	$(1/000)F_1 +$	$1_1$	$(\phi, 0, 0)$	$F_1$	$I4_x/m_x c_{yz} m_y$
	$(1/00a)F_1 +$	$1_2$	$(-\phi, 0, 0)$		
	$(4_z^+/000)F_1 +$	$2_1$	$(0, \phi, 0)$	$F_2$	$I4_y/m_y c_{zx} m_z$
	$(4_z^+/00a)F_1 +$	$2_2$	$(0, -\phi, 0)$		
	$(4_y^-/000)F_1 +$	$3_1$	$(0, 0, \phi)$	$F_3$	$I4_z/m_z c_{xy} m_x$
	$(4_y^-/00a)F_1$	$3_2$	$(0, 0, -\phi)$		

The symmetry group  $J_{ij}$  of an unordered DP consists of symmetry elements  $f \in F_{ij} = F_i \cap F_j < G$ , that leave both DSs, i.e.,  $S_i$  and  $S_j$  unchanged, united with all transposing operations  $\hat{j}_{ij} \in G$ , that simultaneously exchange  $S_i$  and  $S_j$ . Thus, we can write

$$J_{ij} = F_{ij} \cup \hat{j}_{ij} F_{ij} \quad (4)$$

The group  $J_{ij}$  can be treated as a dichromatic (e.g., black and white) space group [22]. If we color the DSs, the symmetry elements  $\in F_{ij}$  are color preserving, whereas all symmetry elements  $\in \hat{j}_{ij} F_{ij}$  (marked with a “hat”) are color changing.

### A. Translational domain pairs

Translational DPs consist of two DSs that share the same orientational state, but differ in their translational state. It can be easily seen that all three translational DPs  $\{1_1, 1_2\}$ ,  $\{2_1, 2_2\}$ , and  $\{3_1, 3_2\}$  are symmetrically equivalent. Indeed, they can be transformed into each other (see Table II) by  $(4_z^+/000)\{1_1, 1_2\} = \{2_1, 2_2\}$ ,  $(4_z^-/000)\{1_1, 1_2\} = \{3_1, 3_2\}$ , and  $(4_x^+/000)\{2_1, 2_2\} = \{3_1, 3_2\}$ , respectively.

In the following we will consider the DP  $\{3_1, 3_2\}$  in some detail, to compare our results with previous calculations [9,12] that have been done for such orientation. Since a DP corresponds to an overlap of *homogeneous* DSs coexisting independently of each other in whole real space, we can represent the DP  $\{3_1, 3_2\}$  in order-parameter (OP) space as  $\{(0, 0, \phi), (0, 0, -\phi)\}$ . As shown in Ref. [17], the symmetry elements that leave a DP invariant can be easily found by inspecting how the order-parameter (OP) components transform under the action of the irreducible representation (Table I).

The symmetry elements that leave  $3_1$  and  $3_2$  unchanged thus form the symmetry group  $F_{3_1, 3_2} = F_3 = I4_z/m_z c_{xy} m_x$ . Those symmetry elements that simultaneously exchange  $3_1$  and  $3_2$  (color changing operations) are given by  $(0, 0, a)F_3$ . Thus, the symmetry group of the DP  $\{3_1, 3_2\}$  can be written as

$$J_{3_1, 3_2} = F_3 + (0, 0, a)F_3 \\ = I4_z/m_z c_{xy} m_x + (0, 0, a)I4_z/m_z c_{xy} m_x. \quad (5)$$

### B. Orientational domain pairs

Pure orientational (ferroelastic) DPs consist of two DSs that share the same translational state, but differ in their orientational state. Interestingly enough, all orientational DPs  $\{S_i, S_j\}$   $i \neq j$  ( $i, j = 1-6$ ) are equivalent. To make contact with other theoretical work [9,15] on ferroelastic DWs in SrTiO<sub>3</sub> we consider here the orientational (ferroelastic) DPs  $\{1_1, 2_1\}$  and  $\{1_1, 2_2\}$ . Note that  $\{1_1, 2_1\}$  is a pure orientational

DP, whereas the DP  $\{1_1, 2_2\}$  differs in orientational *and* translational state and will be called a *mixed* DP [23].

Inspecting Table I one can easily find the symmetry elements  $F_{1_1, 2_1} = F_1 \cap F_2$  which leave  $1_1$  and  $2_1$  unchanged. They consist of those operations which keep invariant  $(\phi, 0, 0)$  and  $(0, \phi, 0)$ . Those elements which simultaneously exchange (color changing operations)  $1_1$  and  $2_1$  transform  $(\phi, 0, 0) \leftrightarrow (0, \phi, 0)$ . They are collected in the set  $\hat{j}_{1_1, 2_1} F_{1_1, 2_1}$ .

Thus, we can write

$$J_{1_1, 2_1} = F_{1_1, 2_1} + \hat{j}_{1_1, 2_1} F_{1_1, 2_1} \\ = \{(1/000) (\bar{1}/000) (m_z/00a) (2_z/00a) \\ (\hat{2}_{\bar{xy}}/00a) (\hat{2}_{xy}/000) (\hat{m}_{\bar{xy}}/00a) (\hat{m}_{xy}/000)\}. \quad (6)$$

For the DP  $\{1_1, 2_2\} \equiv \{(\phi, 0, 0), (0, -\phi, 0)\}$  we get, using Table I,

$$J_{1_1, 2_2} = F_{1_1, 2_2} + \hat{j}_{1_1, 2_2} F_{1_1, 2_2} = \\ = \{(1/000) (\bar{1}/000) (m_z/00a) (2_z/00a) \\ (\hat{2}_{\bar{xy}}/000) (\hat{2}_{xy}/00a) (\hat{m}_{\bar{xy}}/000) (\hat{m}_{xy}/00a)\}. \quad (7)$$

### C. Translational domain twins: Antiphase domain boundaries

The symmetry group  $T_{ij}(\mathbf{n}, \mathbf{p})$  of a domain twin (DT) ( $S_i|\mathbf{n}, \mathbf{p}|S_j$ ) at position  $\mathbf{p}$  with the vector  $\mathbf{n}$  oriented normal to the boundary plane is a layer group [24], i.e., a space group with two-dimensional periodicity.

As for the DPs, in the following we will consider such particular DTs which are interesting in the context of some previous work.

Let us first consider a horizontal APB ( $\mathbf{n} = [100]$ ) between the domain states  $3_1$  and  $3_2$ , as sketched in Fig. 4. The corresponding DT is  $(3_1|[001], (0, 0, 0)|3_2)$  or  $(3_1|[001], (\frac{1}{2}, 0, 0)|3_2)$ . The DWs corresponding to such a DT have been called *easy* APBs [9,12], since their presence does not require any disruption in the oxygen position and no distortion of the oxygen octahedra (Fig. 4). Indeed, electron diffraction studies in SrTiO<sub>3</sub> [25] revealed that these APBs are atomistically thin (1–2 unit cells thick) and planar (see Fig. 10 of Ref. [25]), as a result of the structural coherency of the oxygen octahedra. However, interactions between APBs, or between APBs with other defects, APB splitting, etc., as shown, e.g., in Fig. 4 of Ref. [10] can lead to deviations from the planar shape. In this sense, our approach here—assuming planar domain walls—is an approximation.

The other prominent orientation of the APB, which is parallel to the tetragonal axis (with  $\mathbf{n} = [100]$ , Fig. 5) has been called [9,12] *hard* APB, since—for the case of an atomistic

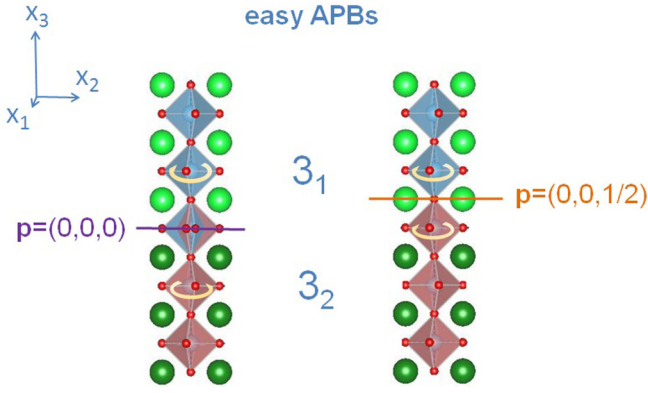


FIG. 4. Schematics of two *easy* APBs ( $\mathbf{n} = [001]$ ) in tetragonal SrTiO<sub>3</sub> at  $\mathbf{p} = (0, 0, 0)$  and  $\mathbf{p} = (0, 0, \frac{1}{2})$ .

thin wall—it could not be drawn without severe distortions of the octahedra. However, hard APBs in SrTiO<sub>3</sub> were found [13] to be about 10 unit cells (ca. 40 Å) thick. In that case the octahedra can rotate smoothly from one DS to the other DS along the domain wall.

The symmetry elements that leave such a twin invariant consist of two parts [26,27]:

$$T_{3_1,3_2} = \bar{F}_3 + \hat{t}_{3_1,3_2} \bar{F}_3, \quad (8)$$

where  $\bar{F}_3$  consists of all operations  $\in F_3$  that leave  $3_1, 3_2, \mathbf{n}, \mathbf{p}$  invariant while  $\hat{t}_{3_1,3_2} \bar{F}_3$  consists of all operations (color changing, marked with hat)  $\in (0, 0, a)F_3$  that simultaneously exchange  $3_1$  and  $3_2$  and transform (at the position  $\mathbf{p}$ )  $\mathbf{n} = [001]$  into  $-\mathbf{n} = [00-1]$  (the latter property is marked by underlining the symbols of such operations). As shown in Ref. [17] the symmetry elements of the layer group of a twin can be conveniently found from the active irrep (Table I), with additionally taking into account how the DW normal  $\mathbf{n}$  transforms at the position  $\mathbf{p}$ . The procedure is described in detail in Ref. [17]. Inspecting the symmetry group  $J_{3_1,3_2}$  together with Table I we find for the translational domain twin

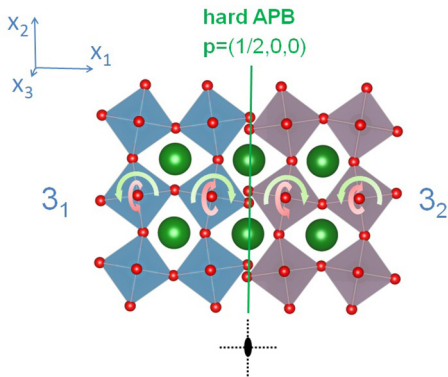


FIG. 5. Representation of a *hard* APB ( $\mathbf{n} = [100]$ ) in tetragonal SrTiO<sub>3</sub> at  $\mathbf{p} = (\frac{1}{2}, 0, 0)$ . The symmetry elements of the layer group of the twin (for a Néel-type wall) are also shown underneath. Note, that in real SrTiO<sub>3</sub> crystals hard APBs are not atomistically thin, but have an extension [13] of about 10 unit cells. This however, does not alter the symmetry elements of the layer group.

(Fig. 4) with  $\mathbf{n} = [001]$  (*easy* APB)

$$\begin{aligned} T_{3_1,3_2}(\mathbf{n} = [001], \mathbf{p} = (000)) &= \mathbf{T}\{(1/000) (4_z^+/000) (4_z^-/000) (2_z/000) \\ &(m_x/0a0) (m_y/0a0) (m_{xy}/0a0) (m_{\bar{xy}}/0a0) \\ &(\hat{2}_x/000) (\hat{2}_y/000) (\hat{2}_{xy}/000) (\hat{2}_{\bar{xy}}/000) \\ &(\hat{1}/0a0) (\hat{m}_z/0a0) (\hat{S}_{4z}^+/0a0) (\hat{S}_{4z}^-/0a0)\}. \end{aligned} \quad (9)$$

The symmetry elements of Eq. (9) form a layer group, i.e., a three-dimensional (3D) space group with 2D periodicity with  $\mathbf{T} = (na, ma, 0)$ ,  $n + m = 2k$ . The corresponding point group is tetragonal, i.e.,  $D_{4h} = 4/mmm$ . From the symmetry elements of  $4/mmm$  we can draw the following conclusion about a possible polarization  $\mathbf{P}(x_3)$  of easy APBs:  $P_1(x_3) = P_2(x_3) = 0$  for  $-\infty \leq x_3 \leq \infty$ , where  $x_3$  defines the position  $x_3 \mathbf{n}$  in the DW. For  $P_3$ , the layer group symmetry, Eq. (9), allows only for odd polarization profiles, i.e., only  $P_3(-x_3) = -P_3(x_3)$  is possible, which implies  $P_3 = 0$  in the center ( $x_3 = 0$ ) of the wall. For comparison, Morozovska *et al.* [9] obtained odd and even solutions from a Landau-Ginzburg-Devonshire (LGD) theory of DWs in SrTiO<sub>3</sub>.

As we have shown in detail in Ref. [17], the layer group symmetry of a domain twin can also be used to get a clue about the order-parameter (OP) profile. Inspecting Table I together with Eq. (9), we find that for easy APBs in SrTiO<sub>3</sub> only one-dimensional solutions are compatible with the layer group symmetry, i.e., those where  $\phi_1(x_3) = \phi_2(x_3) = 0$  and  $\phi_3(-x_3) = -\phi_3(x_3) \neq 0$  (see Fig. 3). Here it is important to note that the layer group symmetry of a twin is independent of the thickness of the corresponding DW, i.e., it is the same for thick and atomistically thin DWs. For this reason we can sketch the profiles of DW properties which are compatible with the corresponding layer group of the twin even if the DW is not infinitely thin.

Following the same procedure as before, we find that the layer group symmetry  $T_{3_1,3_2}$  for easy walls (i.e., with  $\mathbf{n} = [001]$ ) is the same for  $\mathbf{p} = (000)$  and  $\mathbf{p} = (00\frac{1}{2})$ . It is only lowered if we move the center of the wall to a general position  $\mathbf{p} = (00z)$ . In this case, we get  $T_{3_1,3_2}(\mathbf{n} = [001], \mathbf{p} = (00z)) = \mathbf{T}\{1/000 (m_x/0a0)\}$ , which is compatible with  $P_1 = 0, P_2, P_3 \neq 0$ . Since this layer group does not contain symmetry elements (hat and underlined) that simultaneously reverse the domain states and the normal, the corresponding twin is called an “asymmetric twin” [18,26]. Since for asymmetric twins the OP components along the domain wall are not related by symmetry, we shall not consider such a situation further.

Let us now check what happens if we allow for an *additional OP component* to emerge in the vicinity of an easy APB. It is clear that any additional appearance of an OP component (except for special high symmetry points in OP space) can only lower the layer group symmetry of the twin. By combining the layer group methods with order-parameter symmetry as proposed in Ref. [17] we can easily calculate [28] the new symmetry group of the DT and see what restrictions on the components of polarization in the wall are lifted.

Let us start with an easy wall ( $\mathbf{n} = [001]$ ), assuming  $(\phi_1, 0, \phi_3) \rightarrow (\phi_1, 0, -\phi_3)$  along the path (Fig. 3)  $-\infty \leq$

$x_3 \leq \infty$ . Inspecting Table I, we find that the following symmetry elements are compatible with this profile:

$$T_{3,3_2} = \mathbf{T}\{(1/000) (m_y/0a0) (\hat{2}_x/000) (\hat{m}_z/0a0)\}, \quad (10)$$

where  $\mathbf{T} = (na, ma, 0)$ ,  $n + m = 2k$ . A comparison with Eq. (9) shows that the point group symmetry which corresponds to the layer group  $T_{3,3_2}$  is now lowered from  $D_{4h} = 4/mmm$  to the orthorhombic point group  $C_{2v} = mm2$ , which is compatible with  $P_1(-x_3) = P_1(x_3)$ ,  $P_2(x_3) = 0$ , and  $P_3(-x_3) = -P_3(x_3)$ .

However, since it was shown by Tagantsev *et al.* [12], that easy APBs are *stable* against the development of an additional OP component in the wall, this consideration is only of limited interest for *easy* walls. However, it becomes of considerable importance for the case of *hard* APBs, as we shall see in the next part.

Inspecting the symmetry group  $J_{3,3_2}$  of Eq. (5) together with Table I, we find for the translational domain twin at  $\mathbf{p} = (000)$  with  $\mathbf{n} = [100]$  (*hard* APB, Fig. 5), for  $\phi_1 = 0$ ,  $\phi_2 = 0$ ,  $\phi_3 \neq 0$ ,

$$\begin{aligned} T_{3,3_2}(\mathbf{n} = [100], \mathbf{p} = (000)) \\ = \mathbf{T}\{(1/000) (2_x/00a) (m_y/00a) (m_z/000) \\ (\hat{2}_y/000) (\hat{m}_x/000) (\hat{2}_z/00a) (\hat{1}/00a)\}, \quad (11) \end{aligned}$$

where

$$\mathbf{T} = (0, na, ma), \quad n + m = 2k.$$

It is easy to see that the orthorhombic point group ( $D_{2h} = mmm$ ), which corresponds to the layer group  $T_{3,3_2}$  of Eq. (11) is compatible with the polarization components  $P_1(-x_1) = -P_1(x_1)$ ,  $P_2(x_1) = 0$ , and  $P_3(x_1) = 0$ . Moreover, by inspection of Table I we find that the symmetry elements (11) constrain the OP profile to a one-dimensional solution, i.e.,  $(0, 0, \phi_3) \rightarrow (0, 0, -\phi_3)$  along the path  $-\infty \leq \xi \leq \infty$ , which could be called an Ising-type solution.

Very similar symmetry behavior is found for hard APBs at  $\mathbf{p} = (\frac{1}{2}00)$ . The layer group of the corresponding twin forms the same orthorhombic point group symmetry ( $mmm$ ), the profile is constrained to Ising type, and the polarization components are the same as for  $\mathbf{p} = (000)$ .

From these considerations we can conclude that, for the case of a one-dimensional OP profile (Ising walls), APBs in SrTiO<sub>3</sub> are not expected to carry a polarization, regardless of whether they are of hard or easy type.

However, since Tagantsev *et al.* [12] have shown that *hard* APBs in SrTiO<sub>3</sub> develop (already at  $T_c = 105$  K) a component of  $\phi$  perpendicular to the boundary plane, similar to Néel walls in magnetic systems, we want to check how the corresponding symmetry of Eq. (11) is lowered for the case of  $(\phi_1, 0, \phi_3) \rightarrow (\phi_1, 0, -\phi_3)$  along the path  $-\infty \leq x_1 \leq \infty$ .

From Table I we find that, due to the appearance of the component  $\phi_1$  in the wall (see path *N* in Fig. 3), the symmetry (11) is lowered to

$$\begin{aligned} T_{3,3_2}(\mathbf{n} = [100], \mathbf{p} = (000)) \\ = \mathbf{T}\{(1/000) (m_y/00a) (\hat{m}_x/000) (\hat{2}_z/00a)\} \quad (12) \end{aligned}$$

with  $\mathbf{T} = (0, na, ma)$ ,  $n + m = 2k$ . Thus, the appearance of  $\phi_1 \neq 0$  in the vicinity of a hard APB breaks the point-group

symmetry from  $D_{2h} = mmm$  (for  $\phi_1 = 0$ ) to  $C_{2v} = mm2$ , which allows for the development of the (even) polarization component  $P_3(-x_1) = P_3(x_1)$ . The other two components are again constrained by this symmetry to  $P_1(-x_1) = -P_1(x_1)$ ,  $P_2(x_1) = 0$ , as before.

#### D. Orientational domain twins: Ferroelastic domain boundaries

In this section we show the results of our symmetry approach for ferroelastic domain boundaries. To make contact with previous calculations, we will consider here only those orientational twins  $T_{1,2_1}$  (pure orientational) and  $T_{1,2_2}$  (mixed orientational/translational) which correspond to the DPs  $\{1_1, 2_1\}$  and  $\{1_1, 2_2\}$ . In OP space (Fig. 3) the corresponding domain states are represented as points, i.e.,  $1_1 = (\phi, 0, 0)$ ,  $2_1 = (0, \phi, 0)$ , and  $2_2 = (0, -\phi, 0)$ . The domain walls can then be represented as lines which connect the corresponding domain states  $1_1 \rightarrow 2_1$  and  $1_1 \rightarrow 2_2$ .

In other theoretical work [9,15] these twin boundaries (TBs) have been named *hard* TBs or *head-to-head* (HH) TBs and *easy* TBs or *head-to-tail* (HT) TBs. This notation—inspired by the cases of easy and hard APBs—comes from the fact that, for *easy* (HT) TBs, the vector  $\phi = (\phi_1, \phi_2, 0)$  of oxygen octahedra rotations in the DW's center is parallel to the DW normal  $\mathbf{n}$  (Figs. 6 and 7), whereas for *hard* (HH) TBs  $\phi$  is perpendicular to  $\mathbf{n}$  (parallel to the DW plane). For orientational DWs the terms *easy* and *hard* can be misleading, i.e., unlike in APBs they do not correlate with the DW energies. In fact, it was shown [15] that easy TBs can have higher energy than hard ones.

We will show below that the character (easy or hard, HH or HT) of a TB depends on the orientation  $\mathbf{n}$  of the TB ( $[1\bar{1}0]$  or  $[110]$ ), and also on the corresponding DSs, which are connected by the DW. Due to mechanical compatibility [29] there exist two possible orientations of ferroelastic TBs, i.e., with  $\mathbf{n} = [110]$  and  $\mathbf{n} = [1\bar{1}0]$ , respectively. Let us start with a TB [Fig. 7(a)], which connects the DSs  $1_1, 2_1$  with  $\mathbf{n} = [110]$  at  $\mathbf{p} = (000)$ .

The symmetry elements which leave this DT invariant are

$$\begin{aligned} T_{1,2_1}(\mathbf{n} = [110], \mathbf{p} = (000)) \\ = \mathbf{T}\{(1/000) (m_z/00a) (\hat{m}_{xy}/000) (\hat{2}_{xy}/00a)\}, \quad (13) \end{aligned}$$

where  $\mathbf{T} = (-na, na, 2ma)$ .

To check the character (easy or hard) of such a TB, we proceed as follows: Inspecting Fig. 6(a), we find that in OP space the trajectory of this TB leads from  $(\phi, 0, 0)$  to  $(0, \phi, 0)$ , via  $\phi = (\phi, \phi, 0)$  in the TB center (independently of the real path in OP space). Since  $\phi = (\phi, \phi, 0)$  is parallel to  $\mathbf{n} = [110]$ , this is an *easy* (HT) TB. The real space structure of such a TB is shown in Fig. 7(a).

For the TB orientation  $\mathbf{n} = [1\bar{1}0]$ , the rotation vector  $\phi = (\phi, \phi, 0)$  is perpendicular to  $\mathbf{n}$ , implying that the corresponding TB is a *hard* (HH) one. The symmetry elements which leave such a twin invariant are

$$\begin{aligned} T_{1,2_1}(\mathbf{n} = [1\bar{1}0], \mathbf{p} = (000)) \\ = \mathbf{T}\{(1/000) (m_z/00a) (\hat{2}_{xy}/000) (\hat{m}_{xy}/00a)\}, \quad (14) \end{aligned}$$

where  $\mathbf{T} = (na, na, 2ma)$ .

Similarly, one can show that the character of the TB depends also on the domain states. That is, for the twin  $(1_1|2_2)$

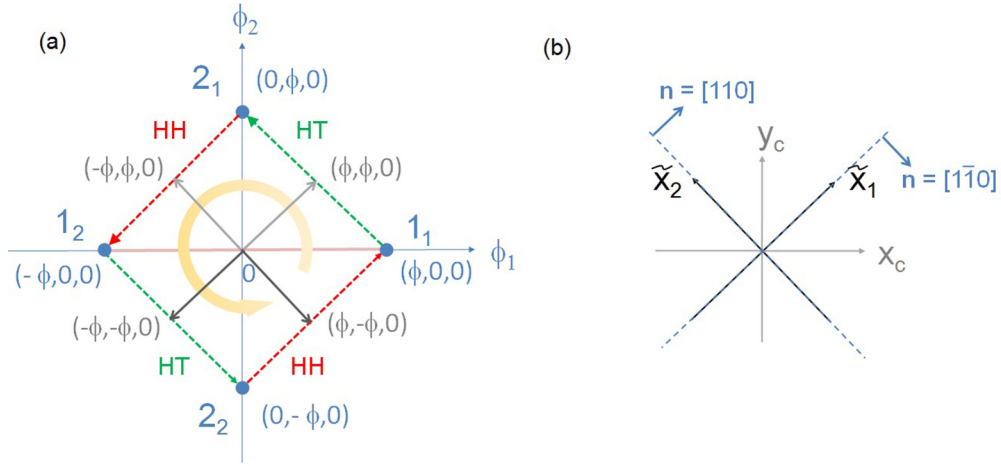


FIG. 6. (a) Representation of four domain states  $1_1, 2_1, 1_2, 2_2$  in order-parameter space, together with a sketch of possible pathways between them, represented as broken lines. The grey arrows indicate the rotation vectors  $\phi$  of oxygen octahedra rotations in the center of the corresponding TB. If such a vector is parallel to the TB normal  $\mathbf{n}$  it is an easy wall, if it is perpendicular to  $\mathbf{n}$ , it is a hard wall. (b) Orientations of ferroelastic TBs in present  $(x_c, y_c, z_c)$  and rotated  $(\tilde{x}_1, \tilde{x}_2, \tilde{x}_3)$  coordinate system.

the OP passes from  $(\phi, 0, 0)$  to  $(0, -\phi, 0)$ , via  $\phi = (\phi, -\phi, 0)$  in the center [Fig. 6(a)]. Thus, for  $(1_1|\mathbf{n} = [110]|2_2)$ ,  $\phi$  is perpendicular to  $\mathbf{n}$ , implying that it is a *hard* (HH) twin boundary [Fig. 7(b)]. The corresponding symmetry of the twin is

$$T_{1_1 2_2}(\mathbf{n} = [110], \mathbf{p} = (000)) = \mathbf{T}\{(1/000) (m_z/00a) (\hat{m}_{xy}/00a) (\hat{2}_{\tilde{xy}}/000)\}. \quad (15)$$

For similar reasons the TB  $(1_1|\mathbf{n} = [1\bar{1}0]|2_2)$  is an *easy* (HT) one and its symmetry elements are

$$T_{1_1 2_2}(\mathbf{n} = [1\bar{1}0], \mathbf{p} = (000)) = \mathbf{T}\{(1/000) (m_z/00a) (\hat{m}_{xy}/000) (\hat{2}_{xy}/00a)\}. \quad (16)$$

## IV. COMPARISON WITH PREVIOUS THEORETICAL RESULTS

### A. Antiphase boundaries

Since the present setting corresponds to the settings of Refs. [9,12], we can directly compare our findings with those previous results. For *easy* APBs, Tagantsev *et al.* [12] found that they are of Ising type ( $\phi_1 = 0, \phi_2 = 0, \phi_3 \neq 0$ ) and stable against the development of any polarization component, i.e.,  $\mathbf{P} = 0$ , in agreement with the present symmetry considerations. By way of contrast, hard APBs of the Néel type ( $\phi_1 \neq 0, \phi_2 = 0, \phi_3 \neq 0$ ) become unstable [12] with respect to a development of a ferroelectric polarization  $P_3$ . These results are based on a LGD free energy expansion with a set of 22 thermodynamic parameters obtained from experiments. The most important coupling term for ferroelectric

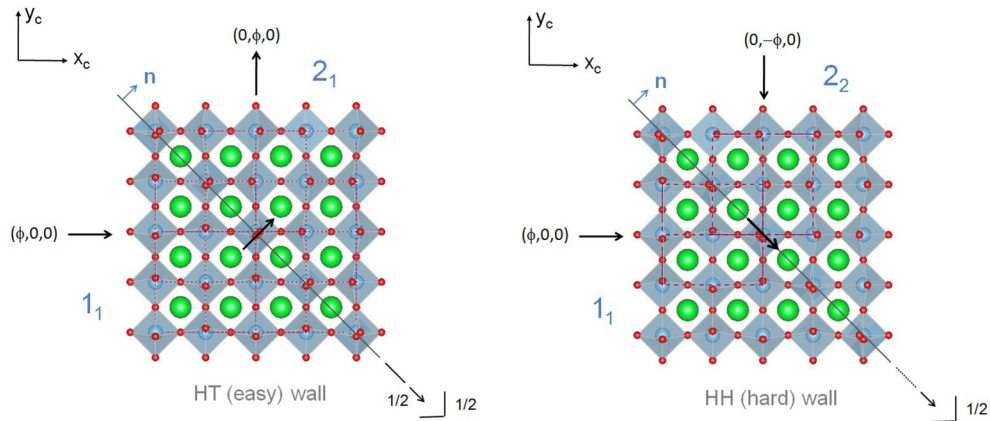


FIG. 7. Representation of two different ferroelastic twins with  $\mathbf{n} = [110]$  at  $\mathbf{p} = (0, 0, 0)$  in tetragonal  $\text{SrTiO}_3$ , together with the symmetry elements of the corresponding layer groups. (a) Pure orientational twin  $(1_1|2_1)$ . The corresponding twin wall is an *easy* (HT) wall. The twin in (b) is of mixed type, i.e.,  $(1_1|2_2)$ , where the corresponding twin wall is a *hard* (HH) one. Note, that the layer group symmetry elements  $(m_{xy}|00a)$  and  $(2_{\tilde{xy}}|000)$  are not clearly visible in the atomistic structure, since only one  $(x, y)$  layer is shown for clarity. The thick black arrows indicate the changes of the vectors  $\phi$  of oxygen octahedra rotations, when passing from one DS to the other one via the corresponding TB. If this vector in the center of the TB is parallel to  $\mathbf{n}$  it is an easy TB, if it is perpendicular to  $\mathbf{n}$  it is a hard one. The character, i.e., *easy* or *hard*, is changed if the orientation of the wall changes from  $\mathbf{n} = [110]$  to  $\mathbf{n} = [1\bar{1}0]$ .

TABLE III. Characterization of the orientational TBs in the two coordinate systems  $(x_1, x_2, x_3)$  and  $(\tilde{x}_1, \tilde{x}_2, \tilde{x}_3)$ , which are rotated by  $45^\circ$  with respect to each other.

TBs	$\mathbf{n} = [110], (\phi_1, \phi_2, \phi_3)$	$\mathbf{n}_r = [100], (\phi_r, \phi_s, \phi_t)$	$\mathbf{n} = [1\bar{1}0], (\phi_1, \phi_2, \phi_3)$	$\mathbf{n}_r = [010], (\phi_r, \phi_s, \phi_t)$
$(1_1 2_1)$	$(\phi, 0, 0) \rightarrow (0, \phi, 0)$ via $(\phi, \phi, 0)$ easy (HT) wall	$(\phi, \phi, 0) \rightarrow (-\phi, \phi, 0)$ via $(0, \sqrt{2}\phi, 0)$ easy (HT) wall	$(\phi, 0, 0) \rightarrow (0, \phi, 0)$ via $(\phi, \phi, 0)$ hard (HH) wall	$(\phi, -\phi, 0) \rightarrow (\phi, \phi, 0)$ via $(\sqrt{2}\phi, 0, 0)$ hard (HH) wall
$(2_1 1_2)$	$(0, \phi, 0) \rightarrow (-\phi, 0, 0)$ via $(-\phi, \phi, 0)$ hard (HH) wall	$(-\phi, \phi, 0) \rightarrow (-\phi, -\phi, 0)$ via $(-\sqrt{2}\phi, 0, 0)$ hard (HH) wall	$(0, \phi, 0) \rightarrow (-\phi, 0, 0)$ via $(-\phi, \phi, 0)$ easy (HT) wall	$(\phi, \phi, 0) \rightarrow (-\phi, \phi, 0)$ via $(0, \sqrt{2}\phi, 0)$ easy (HT) wall
$(1_2 2_2)$	$(-\phi, 0, 0) \rightarrow (0, -\phi, 0)$ via $(-\phi, -\phi, 0)$ easy (HT) wall	$(-\phi, -\phi, 0) \rightarrow (\phi, -\phi, 0)$ via $(0, -\sqrt{2}\phi, 0)$ easy (HT) wall	$(-\phi, 0, 0) \rightarrow (0, -\phi, 0)$ via $(-\phi, -\phi, 0)$ hard (HH) wall	$(-\phi, \phi, 0) \rightarrow (-\phi, -\phi, 0)$ via $(-\sqrt{2}\phi, 0, 0)$ hard (HH) wall
$(2_2 1_1)$	$(0, -\phi, 0) \rightarrow (\phi, 0, 0)$ via $(\phi, -\phi, 0)$ hard (HH) wall	$(\phi, -\phi, 0) \rightarrow (\phi, \phi, 0)$ via $(\sqrt{2}\phi, 0, 0)$ hard (HH) wall	$(0, -\phi, 0) \rightarrow (\phi, 0, 0)$ via $(\phi, -\phi, 0)$ easy (HT) wall	$(-\phi, -\phi, 0) \rightarrow (\phi, -\phi, 0)$ via $(0, -\sqrt{2}\phi, 0)$ easy (HT) wall

instability turned out to be the biquadratic ( $P^2\phi^2$ ) one. In a recent paper [13] the authors have basically confirmed these results by zero-kelvin *ab initio* calculations. They have shown that easy APBs in SrTiO<sub>3</sub> are very thin (only 1–2 unit cells thick), the OP profile being indeed of Ising-type, and the DW polarization  $P_3 = 0$ . For the hard walls they found a thickness of about 10 unit cells (ca. 40 Å), and an even polarization distribution  $P_3(x_1) = P_3(-x_1)$ , which perfectly corresponds to their phenomenological results [12]. However, unlike the earlier Landau-Ginzburg theory [12], which yielded that the hard walls are nearly of Néel type ( $\phi_1 \approx |\phi_3|$ ), the *ab initio* calculations indicate that they are rather close to the Ising type ( $\phi_1 \approx 0, \phi_3 \neq 0$ ).

These results are in basic accordance with our calculations. As shown in Eq. (9), the layer group symmetry of easy APBs ( $\mathbf{n} = [001]$ ) is so high that in the center of easy APBs no polarization is allowed. The only possible component which is allowed by this symmetry is the *odd* distribution  $P_3(-x_3) = -P_3(x_3)$ , and  $P_1 = P_2 = 0$ . Morozovska *et al.* [9] obtained the same results for the polarization components by a phenomenological theory including flexoelectric coupling terms, with the exception that they did not discriminate (Fig. 2 of Ref. [9]) between *odd* and *even* distribution of the polarization  $P_3(x_3)$ .

For *hard* APBs ( $\mathbf{n} = [100]$ ) the layer group symmetry (11) is lower than for the easy ones (9). Nevertheless, it still constrains the polarization to be zero in the center, if an Ising-type character of the wall is assumed. Similar to the case of easy APBs, also in this case the only possible polarization distribution is the *odd* one, which is perpendicular to the domain wall, i.e.,  $P_1(-x_1) = -P_1(x_1)$ , and  $P_2 = P_3 = 0$ .

In agreement with the results from previous calculations [9,12], we obtain a DW polarization  $\mathbf{P} \neq 0$  only if we allow for the appearance of an additional OP component  $\phi_1 \neq 0$ , i.e., the hard APB to be of Néel type. In this case the layer group symmetry (11) is lowered to (12) which is compatible with the polarization profile,  $P_1(-x_1) = -P_1(x_1)$  (odd),  $P_2 = 0$ , and  $P_3(-x_1) = P_3(x_1)$  (even). Tagantsev *et al.* [12] did not consider the component  $P_1$ , but, for the important component  $P_3$ , they also obtained [13] the symmetric (even)

solution. However, their finding of a nearly Ising-type character of hard APBs calls for further investigation, since the present layer group approach predicts  $P_3 = 0$  for a strictly one-dimensional Ising wall ( $\phi_1 = 0$ ). It will be interesting to check whether  $P_3$  vanishes for  $\phi_1 \rightarrow 0$ , as our present results suggest.

Morozovska *et al.* [9], for comparison, found also an even solution for  $P_3$  (assuming Néel-type hard APB), whereas for  $P_1$ —similar to the case of easy walls—they did not discriminate between odd and even solutions.

## B. Ferroelastic domain boundaries

In earlier works some authors have introduced a  $45^\circ$  rotated coordinate system [Fig. 6(b)]. Morozovska *et al.* [9] used  $\tilde{x}_1 = \frac{1}{\sqrt{2}}(x_1 + x_2)$ ,  $\tilde{x}_2 = \frac{1}{\sqrt{2}}(-x_1 + x_2)$ , and  $\tilde{x}_3 = x_3$ . The octahedral tilt  $\tilde{\phi} = (\tilde{\phi}_1, \tilde{\phi}_2, \tilde{\phi}_3)$  in the rotated system is then given as  $\tilde{\phi}_1 = \frac{1}{\sqrt{2}}(\phi_1 + \phi_2)$ ,  $\tilde{\phi}_2 = \frac{1}{\sqrt{2}}(-\phi_1 + \phi_2)$ , and  $\tilde{\phi}_3 = \phi_3$ .

Schiaffino and Stengel [15] used a notation where  $\mathbf{r}$  is parallel to the wall and  $\mathbf{s}, \mathbf{t}$  are perpendicular to the wall, implying that  $\phi_s = \tilde{\phi}_1$ ,  $\phi_r = \tilde{\phi}_2$  for  $\mathbf{n} = [110]$  and  $\phi_t = \tilde{\phi}_3 = \phi_3$  (Fig. 6).

Table III gives an overview on the different orientational TBs in SrTiO<sub>3</sub>, together with the OP pathways in normal and rotated coordinate systems. Inspecting Table III, one observes that the results of Ref. [9] for  $90^\circ$  TBs correspond to the situations  $(1_1|2_1)$  (easy TB, HT) and  $(1_2|2_1)$  (hard TB, HH) with  $\mathbf{n} = [110]$ .

Let us now compare the results of these authors with our findings. First of all we notice that the TBs  $(1_1|2_1)$  and  $(1_2|2_1)$  are crystallographically nonequivalent, i.e., there exists no symmetry element  $\in Pm\bar{3}m$  which would transform one TB into the other. Thus, the microscopic structure of the two TBs is different [17] (similar to Fig. 6), which then can lead to distinct properties of, e.g., DW polarization, etc. The layer group symmetries of the two TBs [Eqs. (13) and (15)], constrain the DW polarizations of both types of TBs to  $\tilde{P}_1(-\tilde{x}_1) = -\tilde{P}_1(\tilde{x}_1)$  (odd solution),  $\tilde{P}_2(-\tilde{x}_1) = \tilde{P}_2(\tilde{x}_1)$  (even solution),  $\tilde{P}_3(\tilde{x}_1) = 0$ . Since the point groups which correspond to both layer groups

are the same for both TBs (orthorhombic, i.e.,  $mm2 = C_{2v}$ ), the polarization components are subject to the same symmetry restrictions, i.e., they can differ only in magnitudes. Indeed, in Ref. [9] (see Figs. 4 and S1) the authors obtain even solutions for  $\tilde{P}_2(\tilde{x}_1)$  for easy and hard TBs.

A very interesting result for ferroelastic TBs was recently obtained by Schiaffino and Stengel [15]. These authors found—based on a combination of DFT and Landau theory—that a sequence of two *different* types (HH, HT) of  $90^\circ$  TBs can lead to a macroscopic polarization of the sample (in the direction  $\mathbf{r}$  parallel to the DW). This can be easily understood along the same lines as before. Let us for example take the TB  $(1_1|2_1)$  followed by  $(2_1|1_2)$ . Since, as above, there is no symmetry operation  $\in Pm\bar{3}m$  which transforms the two TBs into each other, both TBs can carry a polarization component  $P_r$  or  $P'_r$  in the same direction  $\mathbf{r}$ , but with different magnitude. Thus, the sequence  $(1_1|2_1|1_2)$  can carry a macroscopic net polarization  $P_m = P_r - P'_r \neq 0$ , even if the single DW contributions are opposite in sign. In Ref. [15] such a sequence of  $90^\circ$  TBs was called an *antiferrodistortive (AFD) cycloid*, due to the fact, that the order parameter  $\phi$  possesses a counterclockwise rotation across the twin walls (with increasing  $s$ ). This cycloidal induced breaking of inversion symmetry due to the rotation of the OP can be nicely seen in OP space [Fig. 6(a)].

An interesting observation is the following: If instead of the sequence  $(1_1|2_1|1_2)$  one would take  $(1_1|2_1|1_1)$ , i.e., two successive pure orientational (HT) TBs (or two HH TBs), then the macroscopic polarization would be strictly zero. This is because any transformation of the twin  $(1_1|2_1)$  into the reversed twin  $(2_1|1_1)$  transforms  $\mathbf{P}_r$  into  $-\mathbf{P}_r$  and the macroscopic polarization  $\mathbf{P}_m = \mathbf{P}_r - \mathbf{P}_r = 0$ . In OP space [Fig. 6(a)] this would mean that the path leads from  $(\phi, 0, 0)$  to  $(0, \phi, 0)$  and back, which then restores the inversion symmetry.

Thus, any sequence which contains two *different* types (HH and HT, i.e., pure orientational and mixed orientational/translational) of  $90^\circ$  TBs can carry a macroscopic polarization  $\mathbf{P}_m = \mathbf{P}_r - \mathbf{P}'_r \neq 0$ . From these considerations, we can conclude that any difference in the magnitudes of  $P_r$  for  $(1_1|2_1)$  and  $P'_r$  for  $(2_1|1_2)$  must be related to the difference in the translational state, i.e., somehow connected to the internal structure and properties of the APBs. Indeed, inspecting Fig. 8(a), one observes that in OP space an APB of Néel type can be seen as a sequence  $(\phi, 0, 0) \rightarrow (\phi, \phi_2, 0) \rightarrow (-\phi, \phi_2, 0) \rightarrow (-\phi, 0, 0)$ , i.e., quite similar to the cycloidal sequence of TBs.

In the following we show, how this behavior is reflected in the coupling terms of the free energy expansion.

## V. DOMAIN WALL SYMMETRY AND ROTOPOLAR COUPLING IN STRONTIUM TITANATE

Schiaffino and Stengel [15] have recently shown that in addition to flexoelectricity a direct *rotopolar* coupling between polarization and the gradients of the oxygen rotations contributes crucially to a macroscopic polarization of a special (cycloidal) sequence of TBs. To show how this rotopolar coupling simultaneously contributes also to the polarization

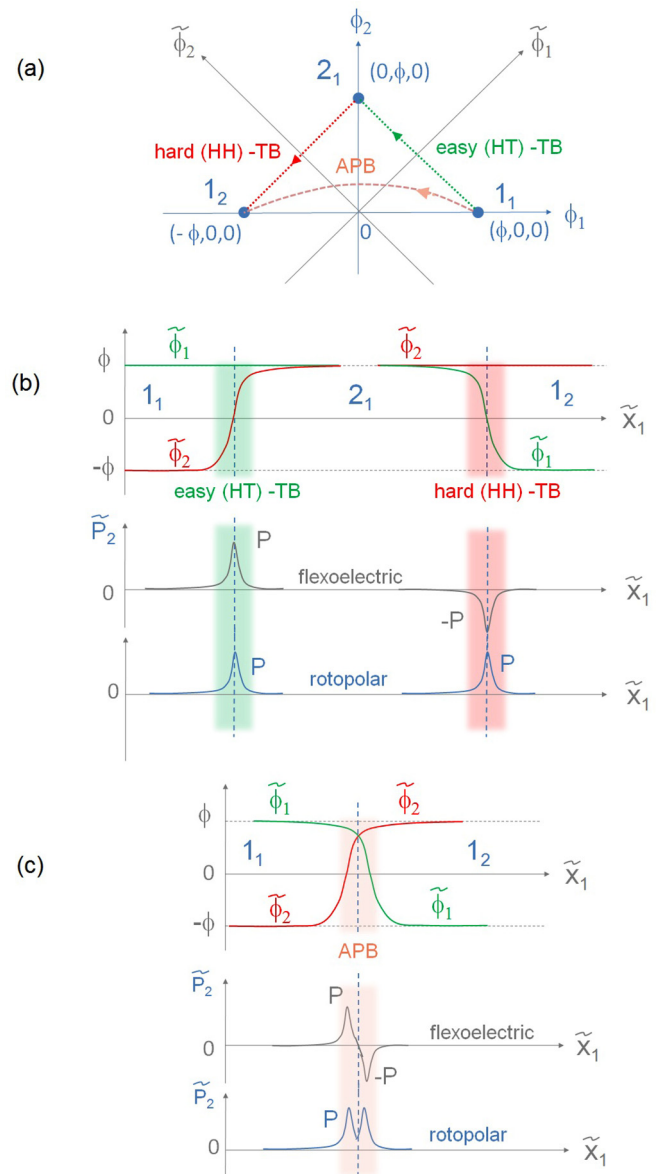


FIG. 8. (a) Sketch of the path between DSs  $1_1 \rightarrow 2_1 \rightarrow 1_2$  in order-parameter space  $(\phi_1, \phi_2, \phi_3)$  and in  $45^\circ$  rotated coordinate system  $(\tilde{\phi}_1, \tilde{\phi}_2, \tilde{\phi}_3)$ . Note that the real trajectory may deviate from this simplified straight lines. An antiphase boundary between the DSs  $1_1$  and  $1_2$  follows approximately the pink broken line, if the boundary is of Néel type. (b) Schematic illustration of the variation of  $\tilde{\phi}_1$  and  $\tilde{\phi}_2$  and the polarization component  $\tilde{P}_2(\tilde{x}_1)$  across the two TBs. Note that the flexoelectric term leads to alternating polarization directions, whereas the rotopolar coupling contributes to  $\tilde{P}_2$  in the same direction in adjacent TBs. (c) An antiphase boundary (APB) of Néel type can be envisaged as a sequence of  $1_1 \rightarrow 2_1 \rightarrow 1_2$ , where the two TBs merge into one APB, i.e., the DS  $2_1$  shrinks to zero. Then the flexoelectric coupling yields an asymmetric contribution  $\tilde{P}_2(-\tilde{x}_1) = -\tilde{P}_2(\tilde{x}_1)$ , whereas the rotopolar term gives a symmetric contribution to the polarization, i.e.,  $\tilde{P}_2(-\tilde{x}_1) = \tilde{P}_2(\tilde{x}_1)$ .

of APBs, we write all corresponding invariants, which are added to the commonly used Landau-Ginzburg free energy expansion  $F_L$  (see, e.g., Ref. [9]) of SrTiO<sub>3</sub>. Using Table I we

find all possible invariants of the type  $W_{ijkl}P_i\phi_k\frac{\partial\phi_l}{\partial x_j}$ :

$$\begin{aligned}
F = F_L + W_1 & \left[ P_1 \left( \frac{\partial\phi_1}{\partial x_3}\phi_3 + \frac{\partial\phi_1}{\partial x_2}\phi_2 \right) + P_2 \left( \frac{\partial\phi_2}{\partial x_3}\phi_3 + \frac{\partial\phi_2}{\partial x_1}\phi_1 \right) + P_3 \left( \frac{\partial\phi_3}{\partial x_1}\phi_1 + \frac{\partial\phi_3}{\partial x_2}\phi_2 \right) \right] \\
& + W_2 \left[ P_1 \left( \frac{\partial\phi_2}{\partial x_2}\phi_1 + \frac{\partial\phi_3}{\partial x_3}\phi_1 \right) + P_2 \left( \frac{\partial\phi_1}{\partial x_1}\phi_2 + \frac{\partial\phi_3}{\partial x_3}\phi_2 \right) + P_3 \left( \frac{\partial\phi_1}{\partial x_1}\phi_3 + \frac{\partial\phi_2}{\partial x_2}\phi_3 \right) \right] \\
& + W_3 \left[ P_1 \left( \frac{\partial\phi_3}{\partial x_1}\phi_3 + \frac{\partial\phi_2}{\partial x_1}\phi_2 \right) + P_2 \left( \frac{\partial\phi_3}{\partial x_2}\phi_3 + \frac{\partial\phi_1}{\partial x_2}\phi_1 \right) + P_3 \left( \frac{\partial\phi_1}{\partial x_3}\phi_1 + \frac{\partial\phi_2}{\partial x_3}\phi_2 \right) \right] \\
& + W_4 \left[ P_1 \frac{\partial\phi_1}{\partial x_1}\phi_1 + P_2 \frac{\partial\phi_2}{\partial x_2}\phi_2 + P_3 \frac{\partial\phi_3}{\partial x_3}\phi_3 \right]. \tag{17}
\end{aligned}$$

Interestingly enough, there are four independent invariants of the type  $W_{ijkl}P_i\phi_k\frac{\partial\phi_l}{\partial x_j}$ , since by symmetry  $W_{1111} = W_{2222} = W_{3333} \equiv W_4$ ,  $W_{1122} = W_{2211} = W_{1133} = W_{3311} = W_{2233} = W_{3322} \equiv W_3$ ,  $W_{1212} = W_{1313} = W_{2121} = W_{2323} = W_{3131} = W_{3232} \equiv W_2$ , and  $W_{1331} = W_{1221} = W_{2332} = W_{2112} = W_{3113} = W_{3223} \equiv W_1$ . Remaining components are 0. In the symmetric case,  $W_1 = W_2$ , the invariants reduce to the type  $W_{ijkl}P_k\frac{\partial(\phi_i\phi_j)}{\partial x_l}$ , i.e., only flexoelectricity comes into play. As will be shown below, the asymmetric case  $W_1 \neq W_2$  provides an additional rotopolar term, that leads to the polarization of cycloidal ferroelastic DWs and APBs in SrTiO<sub>3</sub>.

In the following we will restrict our calculations to the sequence (1<sub>1</sub>|2<sub>1</sub>) and (2<sub>1</sub>|1<sub>2</sub>) with TB orientation  $\mathbf{n} = [110]$ , which corresponds to the case of a HT wall followed by a HH wall. Then, only the OP variables  $(\phi_1, \phi_2, 0)$  are contributing and spatial variations in OP and polarization  $\tilde{P}_2(\tilde{x}_1)$  occur only perpendicular to the wall, which in the rotated coordinate system  $(\tilde{x}_1, \tilde{x}_2, \tilde{x}_3)$  corresponds to  $\tilde{x}_1$  (Fig. 8). In the rotated coordinate system the relevant part of Eq. (17) boils down to

$$\begin{aligned}
F = F_L + 2(W_1 - W_2)\tilde{P}_2 & \left[ \tilde{\phi}_1 \frac{\partial\tilde{\phi}_2}{\partial\tilde{x}_1} - \tilde{\phi}_2 \frac{\partial\tilde{\phi}_1}{\partial\tilde{x}_1} \right] \\
& + 2(W_4 - W_3)\tilde{P}_2 \left[ \tilde{\phi}_1 \frac{\partial\tilde{\phi}_2}{\partial\tilde{x}_1} + \tilde{\phi}_2 \frac{\partial\tilde{\phi}_1}{\partial\tilde{x}_1} \right]. \tag{18}
\end{aligned}$$

The first coupling term  $\propto(W_1 - W_2)$  is the rotopolar term (with *minus*) found by Schiaffino and Stengel [15]. After minimization of the free energy one obtains the following contribution to the polarization  $\tilde{P}_2$ :

$$\tilde{P}_2(\tilde{x}_1) \propto (W_1 - W_2) \left[ \tilde{\phi}_1 \frac{\partial\tilde{\phi}_2}{\partial\tilde{x}_1} - \tilde{\phi}_2 \frac{\partial\tilde{\phi}_1}{\partial\tilde{x}_1} \right]. \tag{19}$$

It yields the same magnitudes and signs for  $\tilde{P}_2$  of adjacent DWs [Fig. 8(b)], and vanishes if  $W_1 = W_2$ .

The second coupling term in Eq. (18)  $\propto(W_3 - W_4)$ , which could be called a flexo-rotocoupling, originates from the well known flexoelectric coupling term  $f_{ijkl}P_k\frac{\partial u_{ij}}{\partial x_l}$ . Since the spontaneous strain due to rotostriction is proportional to [9]  $u_{ij} = R_{ijmn}\phi_m\phi_n$ , the flexoelectric term reads  $f_{ijkl}R_{ijmn}P_k\frac{\partial}{\partial x_l}(\phi_m\phi_n) = f_{ijkl}R_{ijmn}P_k(\phi_m\frac{\partial\phi_n}{\partial x_l} + \phi_n\frac{\partial\phi_m}{\partial x_l})$ , which leads to

$$\tilde{P}_2(\tilde{x}_1) \propto (W_4 - W_3) \left[ \tilde{\phi}_1 \frac{\partial\tilde{\phi}_2}{\partial\tilde{x}_1} + \tilde{\phi}_2 \frac{\partial\tilde{\phi}_1}{\partial\tilde{x}_1} \right]. \tag{20}$$

The important point is that this term is symmetric (i.e., with *plus*) and leads (Fig. 8) to opposite polarization  $\tilde{P}_2$  of adjacent TBs, irrespectively whether they are pure orientational or mixed TBs. From Fig. 8 it becomes clear how such an arrangement of ferroelastic twins can lead to a macroscopic polarization, i.e., the flexoelectric contributions of consecutive twin walls cancel, whereas the rotopolar ones add.

As Fig. 8 shows, the rotopolar coupling may also act as an important mechanism for polarization of APBs.

To show it more clearly, let us return to the APB (3<sub>1</sub>|3<sub>2</sub>) with  $\mathbf{n} = [100]$  (Fig. 5) for which the polarization components in the DW have been calculated [9,12] earlier by Landau-Ginzburg theory. For such geometry the coupling terms of Eq. (17) reduce to

$$F = F_L + P_3 \left( W_1 \frac{\partial\phi_3}{\partial x_1}\phi_1 + W_2 \frac{\partial\phi_1}{\partial x_1}\phi_3 \right). \tag{21}$$

Here we have included only terms which couple to the polarization component  $P_3$ , i.e., in the direction of the wall. In addition there is also a coupling to  $P_1$ . It would lead to  $P_1(-x_1) = -P_1(x_1)$ , in agreement with the layer group results. There is no coupling to  $P_2$  for this geometry, thus  $P_2 = 0$ , also in agreement with the present symmetry analysis [Eq. (12)].

Similar to the ferroelastic cycloid, Eq. (21) can be split into a rotopolar  $[\propto(W_1 - W_2)]$  and a flexoelectric  $[\propto(W_1 + W_2)]$  contribution

$$\begin{aligned}
F = F_L + \frac{1}{2}(W_1 - W_2)P_3 & \left( \frac{\partial\phi_3}{\partial x_1}\phi_1 - \frac{\partial\phi_1}{\partial x_1}\phi_3 \right) \\
& + \frac{1}{2}(W_1 + W_2)P_3 \left( \frac{\partial\phi_3}{\partial x_1}\phi_1 + \frac{\partial\phi_1}{\partial x_1}\phi_3 \right). \tag{22}
\end{aligned}$$

After minimization of the free energy (22) we obtain

$$\begin{aligned}
P_3 \propto (W_1 - W_2) & \left( \frac{\partial\phi_3}{\partial x_1}\phi_1 - \frac{\partial\phi_1}{\partial x_1}\phi_3 \right) \\
& + (W_1 + W_2) \left( \frac{\partial\phi_3}{\partial x_1}\phi_1 + \frac{\partial\phi_1}{\partial x_1}\phi_3 \right). \tag{23}
\end{aligned}$$

In Fig. 9 we show a sketch of the contributions to the polarization profile according to Eq. (23). These plots were made by assuming [Fig. 9(b)] a typical kink-type solution  $\phi_3(x_1) \propto \tanh(x_1)$  and a bump solution  $\phi_1(x_1) \propto 1/\cosh^2(x_1)$ . We observe that, depending on the values and signs of the coupling coefficients  $W_1$  and  $W_2$ , Eq. (23) leads to a peak or double peak

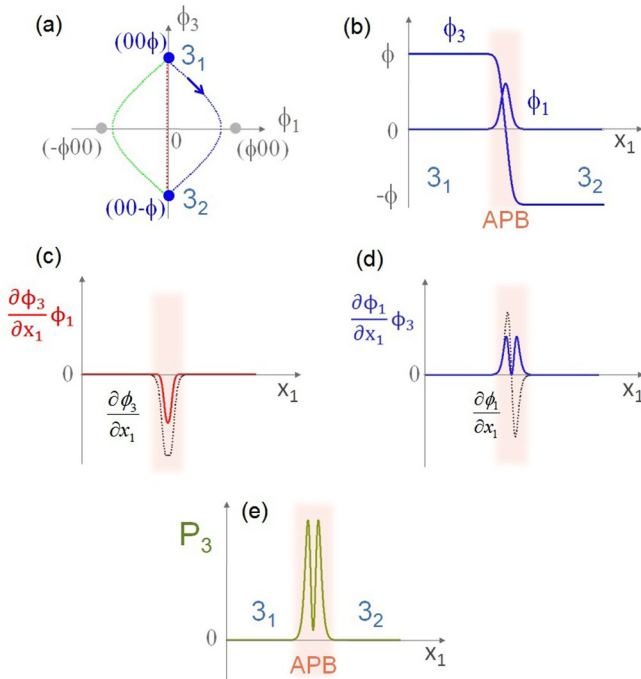


FIG. 9. (a) Schematics of a path between DSs  $3_1$  and  $3_2$  for a Neel-type APB. (b) Sketch of a typical bump ( $1/\cosh^2$ ) and kink ( $\tanh$ ) solution of  $\phi_1(x_1)$  and  $\phi_3(x_1)$ , when crossing a hard (Neel-type) APB ( $3_1|3_2$ ) with  $\mathbf{n} = [100]$ . The derivatives of oxygen octahedra rotations  $\frac{\partial\phi_3}{\partial x_1}$  and  $\frac{\partial\phi_1}{\partial x_1}$  along the path  $x_1$  are shown in (c) and (d) together with the contributions  $\frac{\partial\phi_1}{\partial x_1}\phi_1$  and  $\frac{\partial\phi_1}{\partial x_1}\phi_3$  to DW polarization  $P_3(x_1)$ . The exact final shape of  $P_3(x_1)$  depends on the values and signs of the coefficients  $W_1$  and  $W_2$ . (e)  $P_3(x_1)$  for  $W_2 \gg W_1$ , as found in Ref. [30].

of  $P_3(x_1)$ . In any case  $P_3(x_1)$  is symmetric, in agreement with the corresponding layer group symmetry. In Ref. [30] these contributions were calculated for SrTiO<sub>3</sub> by second-principle methods. Unfortunately, the values of  $W_1$ ,  $W_2$  are not explicitly given there, but the calculated shape (double peak of  $P_3(x_1)$ ) in Fig. 5.5(b) of Ref. [30] leads to the conclusion that for SrTiO<sub>3</sub>,  $W_2 \gg W_1$ , because in that case  $P_3 \propto W_2 \frac{\partial\phi_1}{\partial x_1}\phi_3$  [see Fig. 9(d)]. It also follows from Eq. (23) that the rotopolar and flexoelectric terms contribute to  $P_3$  equally.

## VI. SUMMARY AND CONCLUSION

Summarizing, the present group-theoretical considerations yield polarization profiles of ferroelastic TBs and APBs in SrTiO<sub>3</sub> that are in excellent agreement with phenomenolog-

ical [9,12] and *ab initio* calculations [13,15]. The results show the advantage of complementing layer group analysis with order-parameter symmetry. In contrast to the crystallographic layer group approach, we can study possible symmetry lowering effects on domain wall properties by switching on specific OP components. In this way we have found that the rotopolar coupling, which was recently identified [15] to contribute to a macroscopic polarization of a cycloidal sequence of ferroelastic TBs, provides an important mechanism also for the polarization in APBs. It leads to a polarization of APBs already below the structural phase transition temperature  $T_s \approx 105$  K, whereas the biquadratic coupling [9] induces a domain wall polarization only around  $T_c^* \approx 50$  K. Which of the presently envisaged coupling terms is dominating cannot be told at present. However, the following observation may be helpful for future investigations: The biquadratic coupling term leads to a single peak of polarization centered around the middle part of the domain wall (see, e.g., Fig. 4 of Ref. [13]), whereas rotopolar coupling can produce a double peak [Fig. 9(e)] of the DW polarization (see, e.g., Fig. 5.5 of Ref. [30]). In fact, a double peak structure of the DW polarization was recently observed [10,11] in APBs of PbZrO<sub>3</sub> and we think it could indeed originate from a rotopolar coupling. However, a detailed symmetry analysis of the problem has to be performed before we can draw some conclusions about the possible origin of APB polarization in PbZrO<sub>3</sub>.

It should be noted that the present symmetry analysis can be readily applied to other DW systems, e.g., PbTiO<sub>3</sub> [31], CaTiO<sub>3</sub> [32], etc. Since the approach is, by construction, close to Landau theory of domain walls, we can classify the domain wall profiles of various tensor properties according to symmetry and compare them with the results obtained, e.g., from Landau-Ginzburg theory. In this way, we can take advantage of both methods, i.e., the crystallographic group theoretical one and the order-parameter concept. The main disadvantage of such symmetry considerations is of course that quantitative results can only be obtained by solving the equations describing the structures and properties of specific domain walls either analytically or numerically. However, as shown impressively [9,12,15] for SrTiO<sub>3</sub> this can be a quite challenging task, and symmetry considerations may thus be helpful.

## ACKNOWLEDGMENTS

The present work was supported by the Austrian Science Fund (FWF) Grant No. P28672-N36. W.S. is grateful for countless in-depth discussions with Vaclav Janovec.

- [1] T. Sluka, A. K. Tagantsev, P. Bednyakov, and N. Setter, *Nat. Commun.* **4**, 1808 (2013).  
 [2] S. Van Aert, S. Turner, R. Delville, D. Schryvers, G. Van Tendeloo, and E. K. H. Salje, *Adv. Mater.* **24**, 523 (2012).  
 [3] H. Yokota, H. Usami, R. Haumont, P. Hicher, J. Kaneshiro, E. K. H. Salje, and Y. Uesu, *Phys. Rev. B* **89**, 144109 (2014).

- [4] H. Yokota, S. Niki, R. Haumont, P. Hicher, and Y. Uesu, *AIP Adv.* **7**, 085315 (2017).  
 [5] E. K. H. Salje, O. Aktas, M. A. Carpenter, V. V. Laguta, and J. F. Scott, *Phys. Rev. Lett.* **111**, 247603 (2013).  
 [6] E. K. H. Salje, M. Alexe, S. Kustov, M. C. Weber, J. Schiemer, G. F. Nataf, and J. Kreisel, *Sci. Rep.* **6**, 1 (2016).

- [7] G. F. Nataf and M. Guennou, *J. Phys.: Condens. Matter* **32**, 183001 (2020).
- [8] G. Catalan, J. Seidel, R. Ramesh, and J. F. Scott, *Rev. Mod. Phys.* **84**, 119 (2012).
- [9] A. N. Morozovska, E. A. Eliseev, M. D. Glinchuk, L. Q. Chen, and V. Gopalan, *Phys. Rev. B* **85**, 094107 (2012).
- [10] X. K. Wei, A. K. Tagantsev, A. Kvasov, K. Roleder, C. L. Jia, and N. Setter, *Nat. Commun.* **5**, 3031 (2014).
- [11] X. K. Wei, C. L. Jia, K. Roleder, and N. Setter, *Mater. Res. Bull.* **62**, 101 (2015).
- [12] A. K. Tagantsev, E. Courtens, and L. Arzel, *Phys. Rev. B* **64**, 224107 (2001).
- [13] A. Kvasov, A. K. Tagantsev, and N. Setter, *Phys. Rev. B* **94**, 054102 (2016).
- [14] E. A. Eliseev, S. V. Kalinin, Y. Gu, M. D. Glinchuk, V. Khist, A. Borisevich, V. Gopalan, L.-Q. Chen, and A. N. Morozovska, *Phys. Rev. B* **88**, 224105 (2013).
- [15] A. Schiaffino and M. Stengel, *Phys. Rev. Lett.* **119**, 137601 (2017).
- [16] Y. Frenkel, N. Haham, Y. Shperber, C. Bell, Y. Xie, Z. Chen, Y. Hikita, H. Y. Hwang, E. K. H. Salje, and B. Kalisky, *Nat. Mater.* **16**, 1203 (2017).
- [17] W. Schranz, I. Rychetsky and J. Hlinka, *Phys. Rev. B* **100**, 184105 (2019).
- [18] V. Janovec and J. Přivratská, *International Tables for Crystallography*, edited by A. Authier (Wiley, New York, 2006), Vol. D, Chaps. 3, 4, pp. 449–505.
- [19] H. Unoki and T. Sakudo, *J. Phys. Soc. Jpn.* **23**, 546 (1967).
- [20] V. Janovec, *Ferroelectrics* **12**, 43 (1976).
- [21] V. Janovec, W. Schranz, H. Warhanek, and Z. Zikmund, *Ferroelectrics* **98**, 171 (1989).
- [22] J. C. Bradley, and A. P. Cracknell, *The Mathematical Theory of Symmetry in Solids* (Clarendon, Oxford, 1972).
- [23] It turns out that there is a close correspondence between pure orientational DPs and mixed DPs with easy (head to tail, HT) and hard (head to head, HH) domain twins.
- [24] B. K. Vainstein, *Modern Crystallography I* (Springer, Berlin, 1981).
- [25] R. Wang, Y. Zhu, and S. M. Shapiro, *Phys. Rev. B* **61**, 8814 (2000).
- [26] V. Janovec, *Ferroelectrics* **35**, 105 (1981).
- [27] Z. Zikmund, *Czech. J. Phys. B* **34**, 932 (1984).
- [28] This is one of the main advantages of the present analysis. In a pure group theoretical treatment of DTs it is not possible to consider effects of additional (to the spontaneous OP) order-parameter components on DW properties.
- [29] J. Sapriel, *Phys. Rev. B* **12**, 5128 (1975).
- [30] C. Escorihuela-Sayalero, Second-Principle Methods for Large-Scale Simulations of Realistic Functional Oxides, Ph.D. thesis, University of Luxembourg, 2019.
- [31] J. C. Wojdel and J. Íñiguez, *Phys. Rev. Lett.* **112**, 247603 (2014).
- [32] P. Barone, D. Di Sante, and S. Picozzi, *Phys. Rev. B* **89**, 144104 (2014).
- [33] K. Momma and F. Izumi, *J. Appl. Crystallogr.* **44**, 1272 (2011).